Gold Bull (2014) 47:83–93
DOI 10.1007/s13404-013-0125-6

ORIGINAL PAPER

Alloying colloidal silver nanoparticles with gold disproportionally controls antibacterial and toxic effects

Sebastian Grade · Jörg Eberhard · Jurij Jakobi · Andreas Winkel · Meike Stiesch · Stephan Barcikowski

Published online: 17 November 2013

Abstract Elemental silver nanoparticles are an effective antibacterial substance and are found as additive in various medical applications. Gold nanoparticles are used due to their optical properties in microscopy and cancer therapy. These advantages might be combined within alloyed nanoparticles of both elements and thereby open new fields of interest in research and medical treatment. In this context, laser ablation of solid alloys in liquid gives access to colloidal silver–gold alloy nanoparticles with a homogeneous ultrastructure. Elemental and alloy silver–gold nanoparticles with increasing molar fractions of silver (50, 80, and 100 %) were produced and stabilized with citrate or albumin (BSA). Particles were embedded in agar at concentrations of 3–100 μg cm^{-3} and tested on clinical relevant *Staphylococcus aureus* regarding their antibacterial properties. Cytotoxic effects were measured within the same particle concentration range using human gingival fibroblasts (HGFib). As expected, a reduced fraction of silver in the nanoalloys decreased the antibacterial effect on *S. aureus* according to the evaluated minimal inhibitory concentrations. However, this decrease turned out stronger than expected by its relative mass per particle, due to the electrochemical, disproportionally high effect of gold on the bioresponse to silver within silver–gold nanoalloy particles. BSA was able to stabilize all colloids and maintain antibacterial activity, whereas sodium citrate reduced antibacterial effects and cytotoxicity even at high nanoparticle concentrations. The alloying of silver with gold by laser ablation in liquid produced nanoparticles with both reduced antibacterial and cytotoxic properties in comparison to silver nanoparticles but still retains the application spectrum of both elements combined in one colloid. In particular, alloying with gold may render silver nanoparticles more biocompatible, and allows bioconjugation via established thiol chemistry.

Keywords AgAu · nanotoxicology · antibacterial · nanocolloids

Introduction

Alloying of metals has been established for centuries in material science and metallurgy, aiming at the optimization of material properties and functionality. Multifunctional materials attract a lot of attention in the rapid developing field of nanotechnology. Investigation and integration of new materials can facilitate new approaches, e.g., in the biomedical field. For such applications materials like silver and gold have already been investigated for years and it is well known that elemental silver releases ions [1], whereas gold is known for its optical properties and adsorption of proteins [2, 3]. Combining both elements in one material, in particular within a nanoparticle, might cause a synergetic effect of the properties and thereby provide an access to new materials with new application possibilities. For example, the use of silver in combination with gold could open new possibilities for the conjugation of antibacterial silver nanoparticles to various thiolated biomolecules via covalent bonding to gold atoms.

Due to their antibacterial properties, silver nanoparticles are increasingly used in different medical applications including antimicrobial coatings or wound dressings [1, 4, 5]. Silver

Electronic supplementary material The online version of this article (doi:10.1007/s13404-013-0125-6) contains supplementary material, which is available to authorized users.

S. Grade (✉) · J. Eberhard · A. Winkel · M. Stiesch
Department of Prosthetic Dentistry and Biomedical Materials Science, Hannover Medical School, Carl-Neuberg-Straße 1, 30625 Hannover, Germany
e-mail: grade.sebastian@mh-hannover.de

J. Jakobi · S. Barcikowski (✉)
Technical Chemistry I; University of Duisburg-Essen and Center for Nanointegration Duisburg-Essen (CENIDE), Universitaetsstrasse 7, 45141 Essen, Germany
e-mail: stephan.barcikowski@uni-due.de

reduces bacterial growth by releasing silver ions, which inhibit enzymatic activity and destroy protein structures on bacterial cell membranes [6, 7]. Silver nanoparticles used in antibacterial implant coatings and surfaces are often embedded in composites or hydrogels, which release the silver ions over time to the adjacent area [8, 9]. Unfortunately, high concentrations of antibacterial silver ions also exhibit cytotoxic effects on eukaryotic cells, making it difficult to establish a possible therapeutic window [10–12]. The cytotoxic effects of silver nanoparticles on eukaryotic cells are described in many studies and the particle concentrations, which cause at least moderate cytotoxicity depend very much on the type of cells used [13–16]. The influence of chemicals, added after (surfactants) or during (reducing agents and capping ligands) nanoparticle synthesis on the silver ion release is an additional factor, which can change the antibacterial and cytotoxic effects of silver. For instance, when bovine serum albumin is added to freshly synthesized, ligand-free silver particles, it significantly reduces the antibacterial effect on different species of bacteria [17].

Gold nanoparticles display only very low cytotoxic effects on eukaryotic cell in comparison to silver [16, 18, 19]. They are known for their strong binding affinity to bovine serum albumin, commonly used as stabilizing agent [20–22] and are responsible for the formation of a protein corona on nanoparticle surfaces [23, 24]. It could be assumed that different gold molar fractions in silver–gold alloy nanoparticles change the binding affinity of BSA to these particles subsequently influencing ion release. Regarding ion release, bimetallic alloys show physical and chemical properties very different from their separate monometallic components [25].

Without using any chemical precursors, ligand-free colloidal nanoparticles can be produced by laser ablation of solid targets in liquids [26, 27]. Hence, toxicological analysis of laser-generated colloids reveals toxicity only for nanoparticles and not for residual chemicals [28, 29], like it is the case with chemically prepared colloids [30, 31]. This method enables ablation of different alloy materials, especially if the targets consist of fully miscible elements such as Ag and Au, or Pt and Ir [32–34]. The availability of any desired Ag/Au ratio in a solid alloy, in combination with its ablation in liquid by lasers, gives access to colloidal alloy nanoparticles with defined compositions [35, 36]. Since it has been recently shown that gold–silver nanoparticle surface patterns designed from co-sputtering of gold with silver showed a silver ion release disproportional to the silver content in the alloy, the question arises whether this effect will also be observed in the bioresponse to nanoparticles [37, 38].

The objective of this study was to understand the biological behavior to the combination of bioactive, ion-releasing silver and noble, protein-adsorbing gold in one nanocolloid. The antibacterial and cytotoxic effects on bacteria and cells for different ratios of gold and silver within the particles were tested. Additionally, the influence of two commonly used stabilizers (albumin and citrate) on colloid aggregation and the bioactivity of all synthesized materials were examined.

Material and methods

Synthesis of NP

The generation of colloidal nanoparticles was achieved by laser ablation of metal foils for silver (99.99 %, Goodfellow GmbH, Germany), gold (99.99 %, Allgemeine Gold und Silberscheideanstalt AG, Germany), and two silver–gold alloys (Ag_4Au and AgAu, 99,99 %, accuracy of composition ±1 wt%, fem Research Institute for Precious Metals and Metals Chemistry, Germany) in citrate and BSA solution (Sigma-Aldrich, Germany). The ablation was carried out in an ablation chamber (volume, 30 ml) and with a liquid layer of 4 mm above the target. The laser beam was coupled into the chamber horizontally to minimize interaction with ablation-process-induced bubbles [39]. The detailed description of the ablation setup can be found in [40]. A picosecond laser (Atlantic 532, Ekspla, Lithuania) with 10-ps pulse duration and pulse energy of 110 μJ at a wavelength of 1,064 nm was used for the nanoparticle generation. The laser beam was scanned (SCANcube® 10, ScanLab AG, Germany) on the target and focused using an F-Theta lens with focal distance of 100 mm.

The nanoparticles will in the following be referred to as: gold nanoparticles (AuNP), silver nanoparticles (AgNP), alloy nanoparticle with a molar silver–gold ratio of 4:1 (Ag_4Au, 68.7 wt% Ag) and alloy nanoparticle with a molar silver–gold ratio of 1:1 (AgAu, 35.4 wt% Ag).

Nanoparticle characterization

Stock solutions of nanoparticles were stored at 8 °C after synthesis. Before experimental use they were ultrasonicated for 30 min at 40 kHz (Elma T710DH, Elma, Germany) and diluted to a NP concentration of 60 μg ml^{-1} with H_2O bidest. The nanoparticles were dropped on copper grids coated with polyvinyl formal (Formvar) and dried in an exsiccator to prevent humidity-induced reactions of silver on the TEM grid, which has recently been reported to occur [41]. Images were taken with a TEM (Morgagni 268, FEI, The Netherlands). Element analysis of alloy nanoparticles was carried out with high-resolution TEM (FEI Tecnai F20, FEI, The Netherlands).

Dynamic light scattering measurements for evaluation of hydrodynamic size of the colloids were carried out with StabiSizer PMX 200 C (Particle Metrix, Germany), whereas TEM micrographs were used for the determination of the primary particle diameter. The number frequency of size distribution was fitted with OriginPro 8.6G (OriginLab, USA), using a log-normal function, and the polydispersity index was

calculated according to DIN ISO 13321 as variance (σ^2) divided by (X_c^2). xA spectrometer (Evolution 201, Thermo Fischer Scientific Inc., USA) covering the spectral range from 190–900 nm and a glass cuvette with 10 mm path length and a volume of 4 ml were used for the ultraviolet–visible (UV–vis) measurements. The mass concentration of the nanoparticles was determined in triplicates for different ablation times using a microgram balance (Precisa 40SM-200A, Precisa Gravimetrics AG, Switzerland) with a 10-μg accuracy.

NP effects on bacteria

The Gram-positive bacterium *Staphylococcus aureus* (DSM 20231, DSMZ, Germany) was cultivated in trypticase soy broth (TSB) medium (Oxoid, UK) over night at 37 °C. The next day, 100 μl of overnight culture was inoculated in 10 ml of fresh TSB medium and cultivated until the exponential growth phase was reached.

Different volumes of ultrasonicated nanoparticles dispersed in H_2O were mixed with liquid Muller–Hinton agar (CM0405, Oxoid, UK) to achieve NP concentrations of 6–100 μg cm^{-3} within the agar. Each plate was filled with 2 ml agar-nanoparticle mixture, which solidified within 15 min. If NP are fully dissolved and released from the agar nanoparticle composite, the total Ag ion dose would be equivalent to 12–200 μg assuming that the volume of such a suspension is constant. *S. aureus* was diluted in phosphate-buffered saline to a concentration of 5×10^3 cells ml^{-1}. Bacteria suspension (100 μl) was plated on agar and incubated overnight at 37 °C. The dosage of Ag^+ ranged between 24 and 400 ng $cell^{-1}$ or 1.6×10^{11} to 2.7×10^{12} silver nanoparticles per bacterial cell in the inoculum. Note that the nanoparticles are immobilized in the agar, so the mass concentration is more relevant than the number concentration. The mass concentration range in the agar gel was selected based on earlier experiences [11]. After 24 h incubation, colony forming units were counted on four plates. It has recently been reported that duration of storage affects the toxicity of AgNP [42]. In order to eliminate such an influence, the experiments were repeated at four different storage intervals after the synthesis of the NP (1, 4, 8, and 16 weeks).

Cytotoxicity

Human gingival fibroblasts (HGFib, catalogue number 121 0412, Provitro, Germany) were cultivated and maintained in Dulbecco's modified Eagle's medium (DMEM) (FG0435, Biochrom, Germany) supplemented with 10 % fetal bovine serum (P270521, Pan-Biotech, Germany), 100 U ml^{-1} penicillin (A2213, Biochrom, Germany), and 100 μg ml^{-1} streptomycin (A2212, Biochrom, Germany) at 37 °C in 5 % CO_2 with 95 % relative humidity. HGFib cells were seeded at a density of 5×10^3 cells per well in 96-well plates for the 3-(4,5-dimethylthiazol-2-yl)-2,5-diphenyltetrazolium bromide (MTT) assay. After 24 h of cultivation, the supernatant was removed, and 100 μl of fresh media containing different amounts of elemental or alloy NPs was added. Therefore, ultrasonicated nanoparticles were diluted in DMEM to NP concentrations of 6–50 μg ml^{-1}, the total theoretical Ag^+ ion dose is equivalent to 0.6–5 μg. The dosage of Ag^+ ranged between 0.12 and 1 ng $cell^{-1}$, or 8.1×10^8 and 6.75×10^9 NP $cell^{-1}$. Note that the nanoparticles are exposed to the cells in the colloidal state. For each concentration of NPs, four wells were incubated at 37 °C for 24 h.

The test for mitochondrial function of HGFib cells was performed by a MTT viability assay according to the protocol of the manufacturer (Cell Proliferation Kit 1, Roche Diagnostics, Switzerland). After 24 h of incubation, 10 μl of staining solution was added to each well. Following 4 h of incubation, the addition of 100 μl of solubilization solution per well caused cell lysis and stain release overnight at 37 °C. The absorbance of the resulting formazan was measured according to the protocol at a wavelength of 540 nm using a fluorescence microplate reader (Infinite F200, Tecan Group, Germany). Since the surface plasmon resonance (SPR) of Au peaks at 520 nm with a significant extinction at 540 nm for increasing amounts of Au in the AgAu-NP, this referencing background signal is important and has to be performed for each Ag and Au content separately. To eliminate the influence of nanoparticle extinction as well, wells with corresponding nanoparticle concentration in a medium without cells were measured as reference. Cell viability was classified into different levels of cytotoxicity according to Sjogren et al. [43]: More than 90 % cell viability was interpreted as noncytotoxic, 60–89 % cell viability as slightly cytotoxic, 30–59 % as moderately cytotoxic, and <30 % as a severely cytotoxic effect.

Statistical analysis

Differences in cytotoxicity between groups of nanoparticles stabilized with BSA and sodium citrate as well as between all particles stabilized by the same agent were tested by Student's *t* test. Statistically significant differences were accepted at a p value of 0.05 and below.

Results and discussion

Characterization of NP

Laser ablation in liquid provides the production of colloidal nanoparticles from bulk material with a homogeneous composition of elements, in particular if the elements are fully miscible like AgAu, PtIr, or NiFe [32, 33, 39]. This method permits the generation of functionalized colloids without chemical precursors [44, 45]. Bovine serum albumin, which

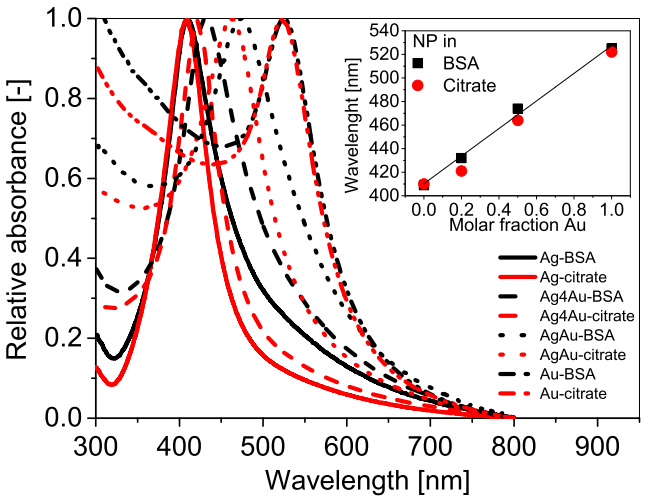

Fig. 1 Validation of alloy composition by plasmon resonance characterization: peak-normalized UV-vis spectra of laser-generated Ag, Ag_4Au, AgAu, and Au nanoparticles in aqueous BSA and citrate solutions

adsorbs on the colloid surface, is often used for studies on nanoparticles and their biological effects [46–48] and sodium citrate is widely used in chemical-based synthesis of both gold and silver nanoparticles so that these ligands were applied in comparison.

The UV–vis analysis of laser-generated nanoparticles confirmed the formation of alloys due to the SPR-contribution of each element [49]. The position of SPR peak (Fig. 1) was linearly red-shifted with an increase in the gold molar fraction between the peaks of pure silver and pure gold. The difference in the SPR-peak position between BSA and citrate stabilized nanoparticles resulted from different refractive indices of these molecules. In contrast to the chemically prepared Ag–Au nanoparticles, which revealed gradients of element distribution [50, 51], the line scan of laser-generated Ag–Au nanoparticles showed a uniform distribution of both elements (Fig. 2). The nanoparticle's ultrastructure is specific for the respective synthesis methods. The laser-based one-step method results in the formation of nanoparticles through condensation of ablated material in a cavitation bubble on a microsecond scale [52, 53], whereas chemical coprecipitation of Ag–Au nanoparticles generally leads to the enrichment of the nobler element (Au) in the nanoparticle core and presenting the less noble element (Ag) at the particle's shell [50]. In Fig. 3, the analysis of TEM micrographs from generated nanoparticles revealed a very similar distribution of primary particle diameter for nanoparticles generated in BSA and citrate solutions (2–4 nm peak size). Calculated from the peak maximum of the lognormal distribution, the size of all BSA-stabilized nanoparticles ranges between 2.3 and 3.5 nm. In comparison to BSA, citrate-stabilized nanoparticles were slightly bigger, between 4.1 and 4.7 nm. The differences in size distribution for BSA and citrate-stabilized nanoparticles can be attributed to higher affinity of BSA to the nanoparticles, which sterically block the surface, preventing further growth. Particle sizes in studies, which investigated biological effects of silver and gold colloids, often cover size ranges including 1–50 nm comparable to the presented results [1, 5, 13, 54, 55].

Stability of colloids in suspension

Xiu et al. showed that the crucial factor for antibacterial and cytotoxic activity of silver colloids is the particle size and subsequently the release of silver ions. Particle morphology influences the biological activity only by changes in their surface to volume ratio [56, 57]. The stabilization of nanoparticles within fluids is an important factor for the characterization of these particles in biological systems. Isolated particles have a higher surface to volume ratio than aggregated particles and release more silver ions. Particle aggregation would reduce the ion release.

We compared two different stabilizing agents often used in the synthesis of nanoparticles, bovine serum albumin and sodium citrate. While the aggregation was high for all species of tested nanoparticles when stabilized with sodium citrate, particles were found dispersed when stabilized with BSA and displayed only little aggregation (Fig. 3). Sodium citrate is a

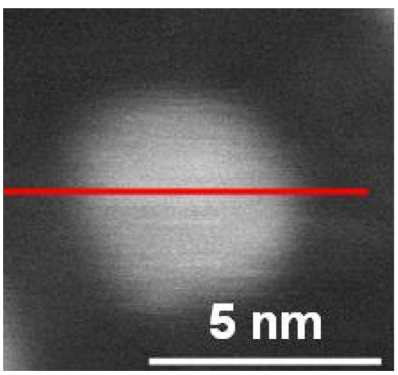

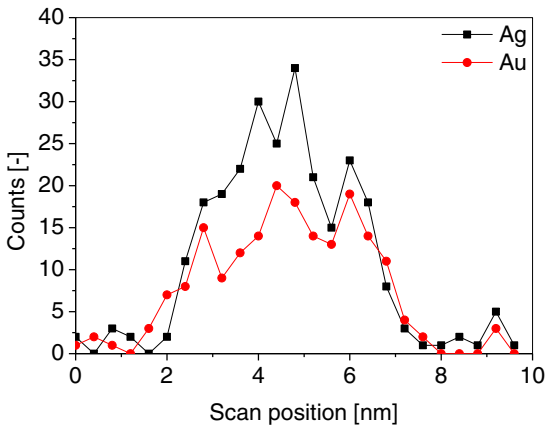

Fig. 2 Ultrastructure of the nanoalloy: TEM-EDX line scan of AgAu nanoparticles generated by pulsed laser ablation of AgAu target in liquid. Data indicate homogeneous, non–segregated, non–core–shell ultrastructure

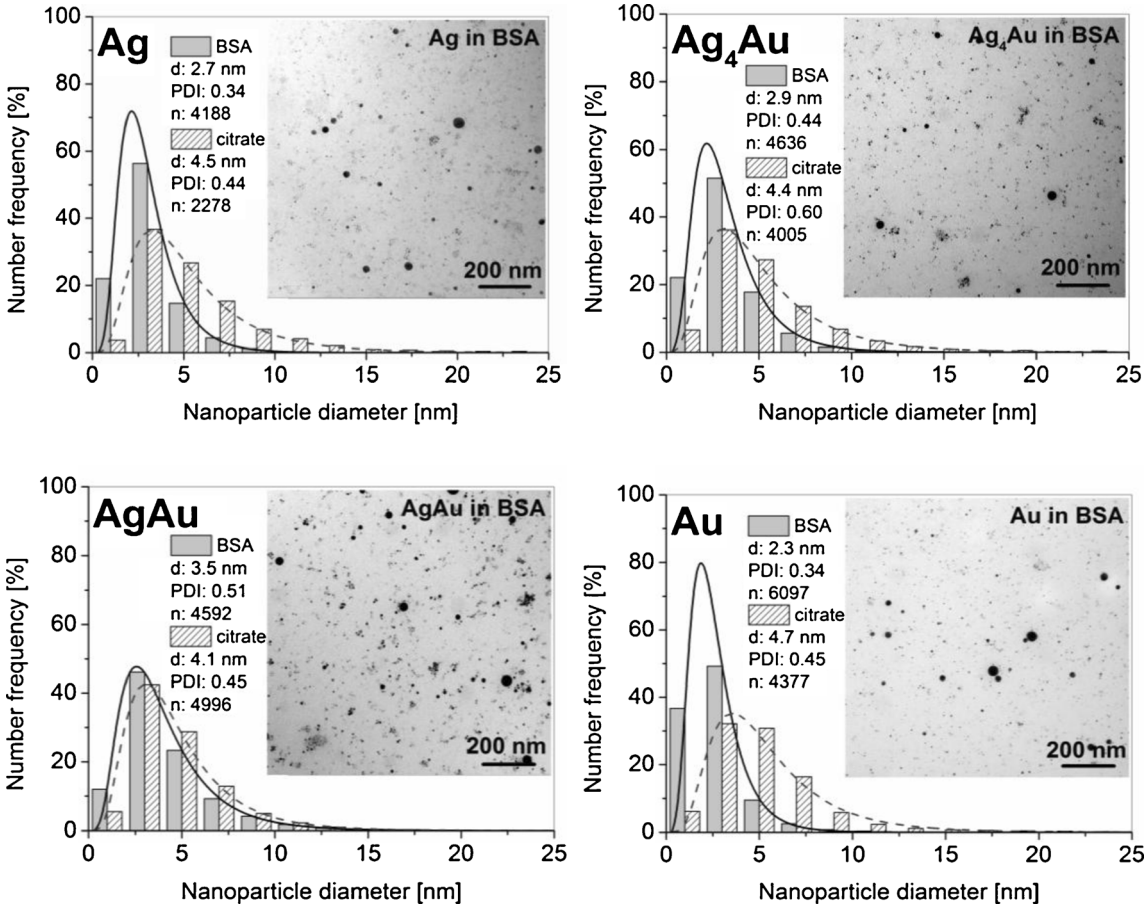

Fig. 3 Nanoparticle diameter histograms and related TEM micrographs of laser-generated Ag, Ag_4Au, AgAu, and Au nanoparticles (BSA samples; for citrate, see Fig. 1 in supporting information, 3d storage in H_2O bidest). Most frequent nanoparticles are in similar size ranges of 2–3 nm (BSA) and 3–4 nm (citrate)

reducing agent and is able to reduce ionic silver to its elemental form. The interaction of released silver ions with citrate molecules, which act as a reductant and stabilizer, is described elsewhere [58]. This induces an equilibrium of dynamic particle growth in the colloid by ripening and dissolution after oxidation due to molecular oxygen present in water. Contrary to steric stabilization with BSA, electrosterically stabilized laser-generated nanoparticles with citrate molecules aggregate on the TEM grid during the drying process (Fig. 3) (Fig. 1 in supporting information).

Over the course of 16 weeks storage, the amount of aggregation is stable. A final state of aggregation for the nanoparticles was already reached after the first days of storage, when the stabilizing effect was insufficient. This aggregation effect of nanoparticles has been described before and explains the reduced antibacterial and cytotoxic effects of silver nanoparticles and both alloys after storage [42, 59]. Using BSA, storage for several weeks was possible without particle aggregation. We assume that bovine serum albumin was an effective agent for all tested elemental and alloy NP to sterically restrict particle aggregation. Note that BSA is a mass component in serum and many cell culture media anyway.

Antibacterial activity of nanoparticles

Biological effects of AgAu alloy nanoparticles have only been tested in a few studies, especially since aqueous synthesis of particles with a homogeneous distribution of gold and silver atoms is difficult to achieve. Previous studies have often been conducted with coated particles synthesized in a coprecipitation method, resulting in a gold core and a silver shell. Recently, particles with a core–shell composition with a higher gold fraction at the particle core and a higher silver fraction on the particle surface were produced by chemical synthesis and analyzed for their biological effects [50, 59].

It could be expected that the release of Ag ions decreases proportionally to the increasing gold molar fraction, due to the change of electrochemical potential [60]. However, disproportional anomalies may take effect on the nanoscale: recently, Alissawi et al. showed that different compositions of AgAu nanoparticles led to different kinetics of ion release and were not proportional to the amount of silver in each composition. This effect was explained by entropy of mixing of AgAu alloys. The immersion of AgAu alloy has shown the highest ion release after 40 min with decreasing release rates after 2h,

Table 1 Minimal inhibitory concentration (MIC) against *S. aureus* and moderately cytotoxic concentration (Tox50) against HGFib of NP with different Ag/Au ratios and stabilizing agents (sodium citrate and BSA)

Colloid and stabilizing agent	NP mass dose		Ag mass in NP dose	
	MIC (μg NP cm^{-3})	TOX 50 (μg NP cm^{-3})	MIC (μg Ag cm^{-3})	TOX 50 (μg Ag cm^{-3})
Ag+BSA	12	9	12	9
Ag+Na citrate	25	29	25	29
Ag_4Au+BSA	25	9	17.2	6.2
Ag_4Au+Na citrate	50	55	34.4	37.8
AgAu+BSA	100	25	35.4	8.9
AgAu+Na citrate	>100	>100	>35.4	>35.4
Au+BSA	>100	>50	NA	NA
Au+Na citrate	>100	>100	NA	NA

1d and 2d. After 1 day of exposure, the ion release changes and increases relative to the silver amount in the alloy. According to these results, the ion release of AgAu nanoparticles could be adjusted to further applications just by variation of the gold molar ratio and nanoparticle sizes[61].

With an increasing ratio of silver, the antibacterial effect of laser-generated nanoparticles on *S. aureus* increased. With the exception of gold and aggregated AgAu (stabilized by sodium citrate), all NP inhibited bacterial growth within the used concentration range from 6 to 100 μg ml^{-1} (Table 1).

Nanoparticles synthesized from pure silver had the strongest antibacterial effect with a complete growth inhibition beginning at a concentration of 12 μg ml^{-1}. The antibacterial effect of silver nanoparticles on *S. aureus* was comparable to other studies examining the biological effects of silver colloids [5, 10, 17]. Taking similar particle sizes into account, a comparable antibacterial effect between laser-generated and chemically synthesized AgNP can be assumed.

Elemental gold nanoparticles synthesized with the described method showed no antibacterial effect within the used concentration range of 6–100 μg cm^{-3}. Interestingly, the antibacterial effect of gold-alloyed AgNP on *S. aureus* decreased much more when the silver ratio within the alloys is taken in consideration.

By decreasing the molar silver fraction in the nanoalloy from 100 % (AgNP) to 80 % (Ag_4Au), the minimal inhibitory concentration (MIC), and therefore the effective concentration of nanoparticles needed to inhibit growth, was increased by 100 % (Table 1). This was observed for both alloys whether stabilized with BSA or sodium citrate. For the AgAu alloy with a 50 % molar silver fraction (equal to 35.4 % of silver mass fraction), the total mass dose of silver was one third of

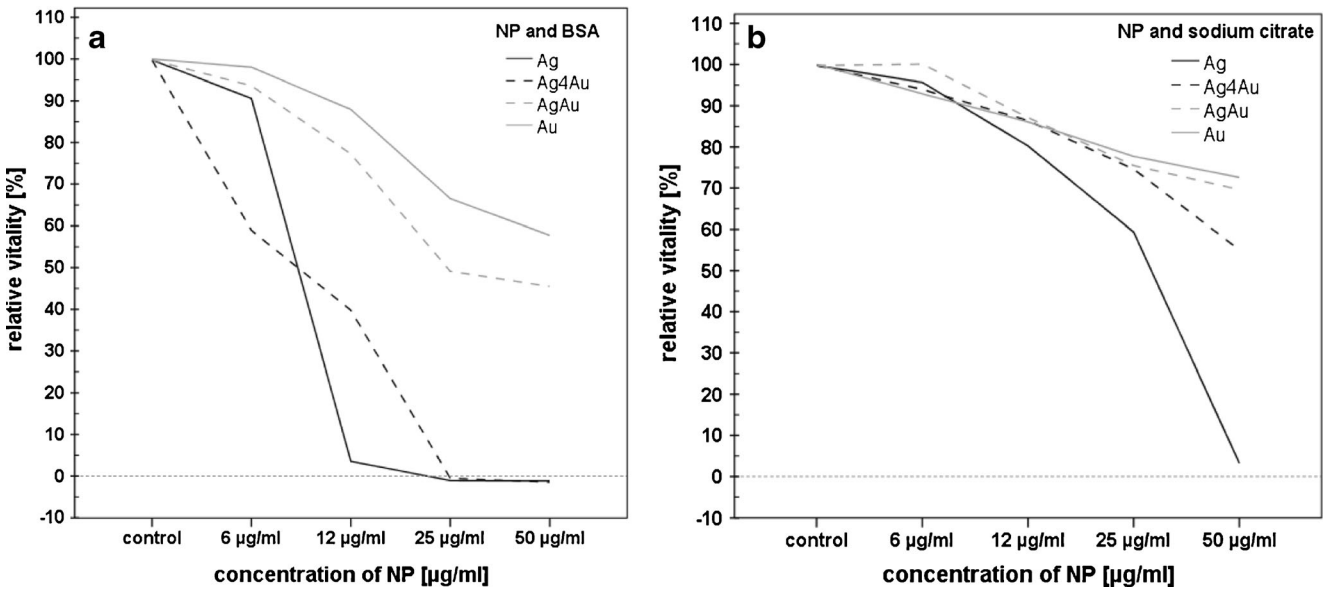

Fig. 4 Influence of nanoparticle composition and mass dose on toxicity: cell viability of human gingival fibroblasts after a treatment with four different elemental and alloy nanoparticles (Ag, Ag_4Au, AgAu, and Au) stabilized with **a** bovine serum albumin and **b** sodium citrate, 50 % relative vitality and lower is set as a threshold for moderate and severe cytotoxicity

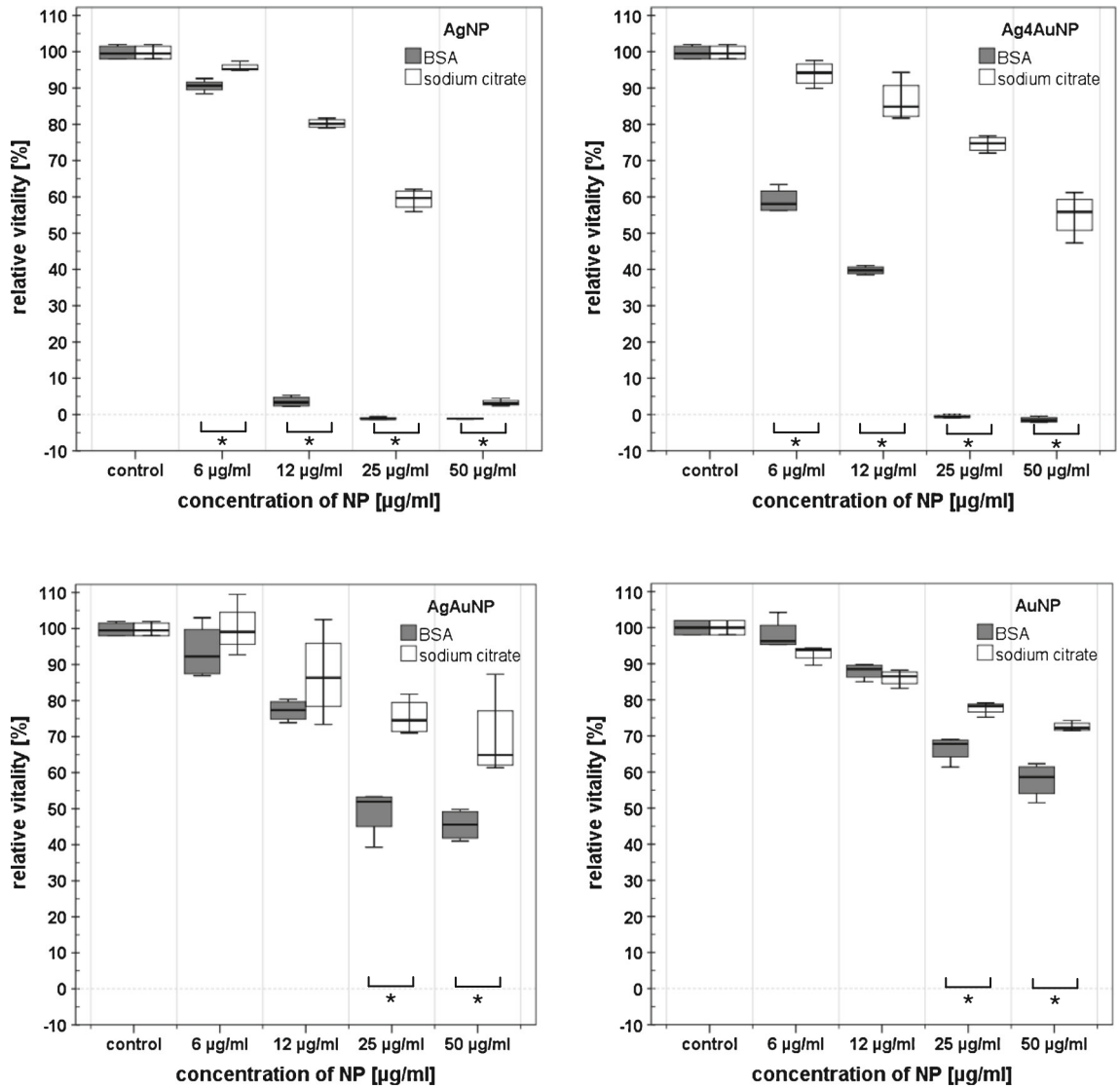

Fig. 5 Cell viability of human gingival fibroblasts after the treatment with four different elemental and alloy colloids (Ag, Au, AgAu, and Ag_4Au) stabilized with bovine serum albumin and sodium citrate (statistically significant differences between both groups of stabilizers, $p < 0.05$)

the pure silver particles, but the MIC was eight times higher than for the particles stabilized by BSA. This reduction of the antibacterial effect was unexpected considering the total silver dose. Physicochemical properties of gold and silver could be the reason for this effect. Beside the kinetic effect, which was described by Alissawi et al. [37], a second effect that may influence silver ion release could be discussed. Since BSA chemisorption to gold surfaces via cysteine or disulfide moieties is more pronounced with an increase of the gold fraction, the protein corona will be more distinct [23, 24]. This effect may sterically hinder the ion release. Differences between bovine serum albumin and sodium citrate regarding their function as stabilizers of antibacterial effects were distinct. Nanoparticles stabilized by sodium citrate had to be used in a twofold concentration to achieve the same reduction in bacterial growth compared to NP stabilized by BSA. In consideration of the differences in aggregation state between nanoparticles stabilized with BSA and sodium citrate, the lower effect of bacterial growth reduction can be attributed to reduction properties of citrate, which provoke reduction of bio active silver ions to elemental silver [50]. Furthermore, primary particles in suspension feature a higher surface/volume ratio than aggregated colloids and release more silver ions at the same silver concentration [62]. After a storage time of 16 weeks and repetition of the cell culture experiments, most particles showed the same threshold concentration at which the bacterial growth was inhibited completely (Fig. 2, Table 2 in Supplementary info).

In summary, BSA stabilized and preserved the antibacterial effect of pure Ag and both nanoalloys more efficiently compared to sodium citrate. Alloying silver with gold caused biological deactivation of a disproportionally high silver fraction in alloy nanoparticles.

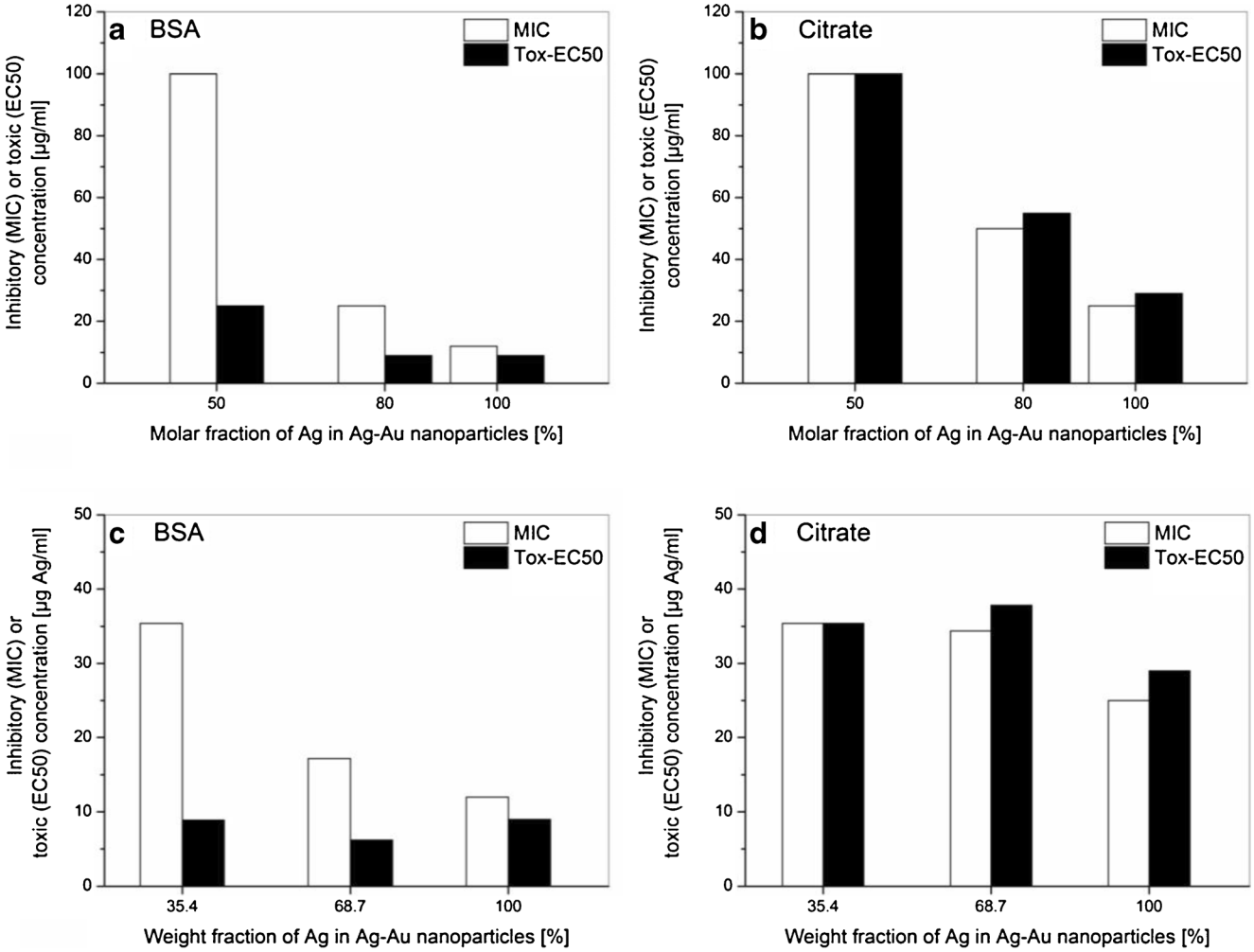

Fig. 6 Silver dosage dependent cell viability of human gingival fibroblasts **a**, **b** and antibacterial activity on *S. aureus* **c**, **d** after treatment with three different nanocolloids (Ag, AgAu, Ag4Au) stabilized with **a**, **c** bovine serum albumin and **b**, **d** sodium citrate

Cytotoxicity of NP

Cytotoxicity of silver nanoparticles was described in many studies, but the mechanisms of particle–cell interactions negatively affecting cell viability are manifold and complex [16]. Differences in particle size, charge, and cell type can show very variable results [63]. It was described in former studies that laser-generated silver NPs had strong cytotoxic effects on HGFib comparable with nanoparticles synthesized by other methods [10]. Severe cytotoxicity was reached at the same concentration of nanoparticles as reported widely in literature [1].

In the present study, cytotoxicity was measured with an MTT assay, which depicts the metabolic activity of the HGFib. Comparing BSA and sodium citrate, statistically significant differences regarding their influence on cytotoxicity of nanoparticles were found. In accordance with the result for antibacterial activity, particles stabilized by BSA showed a stronger effect on cell metabolic activity particles stabilized by the reducing agent sodium citrate. Nanoparticles combined with BSA kept their cytotoxic effect, but colloids with sodium citrate showed a statistically significant reduction of cytotoxicity.

After 1 week storage, silver nanoparticles stabilized with BSA showed—deriving from a reduced metabolic activity—a slightly cytotoxic effect at a concentration of 6 µg ml^{-1} and severe cytotoxicity at 12 µg ml^{-1}. This steep decrease in cell survival ended at 25 µg ml^{-1} where all metabolic activity of HGFib was completely stopped. After 16 weeks of particle storage, the AgNP showed a decreased effect on cell survival with now only moderate cytotoxicity at 12 µg ml^{-1}. But even here, death of all cells was observed at 25 µg ml^{-1} (data for 4, 8, and 16 weeks shown in Fig. 3a–h in supplementary data).

Silver nanoparticles stabilized with sodium citrate showed a cytotoxic effect only at higher concentrations of nanoparticles (Fig. 4). They showed also a slightly cytotoxic effect on HGFib at concentrations of 6 to 25 µg ml^{-1}. At a NP concentration of 50 µg ml^{-1}, a severe effect on cell viability was

measured. After longer storage, no complete cell death was observable even at 50 μg ml^{-1}. Again, differences in cytotoxic effects between nanoparticles stabilized with BSA and sodium citrate can be explained in accordance with the statement for antibacterial activity.

Elemental gold NP showed a moderate cytotoxicity at concentration of 25 μg ml^{-1} and higher, which is reported by other authors. They described the ability of AuNP to enter the cell nucleus of cells and subsequently interacting with proteins and enzymes within cells [16, 64].

The reduction of silver-related effects by alloying Ag with Au on the nanoscale was also observed for cytotoxicity. With an increasing fraction of gold within the nanoparticles the cytotoxic effect was reduced more strongly than expected if the silver mass dose would be taken into account as the bioactive component (Figs. 5 and 6).

Ag_4Au stabilized with BSA showed also a decrease in cell viability with higher concentrations of nanoparticles, but the decrease was less severe than for pure AgNP. Strong cytotoxicity was first observed at a NP concentration of 25 μg ml^{-1}, after 16 weeks of storage there cytotoxicity was reduced. Nanoparticles stabilized by sodium citrate showed only a small decrease in cell vitality even at higher concentrations of NP. At 50 μg ml^{-1}, there was only a moderate cytotoxicity.

The cytotoxic effect of the alloy AgAu was similar to Ag_4Au. A severe reduction of cell survival would have been expected at a concentration of 34 μg ml^{-1} of AgAu, which would contain the same silver mass as pure silver NP at a concentration of 12 μg ml^{-1}. Interestingly, even at 50 μg ml^{-1}, the nanoparticles had only a moderately cytotoxic effect on HGFib. Especially AgAu particles stabilized by sodium citrate showed a similar curve compared to Ag_4Au. Overall, bioactivity of Ag nanoparticles is significantly decreased by alloying with Au. A given mass dose of Ag is more effective if presented as elemental Ag compared to an Ag equivalent higher mass dose of AgAu alloy nanoparticles (Figs. 5 and 6). Hence, the electrochemical series and redox potential of Ag and Au is not expected to be the only influencing factor.

These effects were also described by other studies, which used chemically prepared gold–silver alloy nanoparticles [59]. However, both studies used alloy colloids with a core to shell increase in the silver ratio and explained the reduced cytotoxic effects with this heterogenic ultrastructure of the particles. In our case, homogeneous ultrastructure has been observed for Ag–Au alloy fabricated by laser ablation in liquid [65] and has also been reported into detail for other metal alloy nanoparticles fabricated by laser ablation [34]. In consequence, heterogeneity cannot be taken as explanation. Based on findings from the literature, we speculate that entropy of mixing [37] and effect of protein corona affected the silver ion release [23, 24].

Conclusion

Silver–gold alloy nanoparticles with a homogeneous ultrastructure and comparable size were analyzed for their biological activity and compared to elemental Ag und Au nanoparticles. Both antibacterial and cytotoxic effects decreased disproportionately with increasing fraction of gold indicating a physicochemical interaction between both elements. It is evident that gold has a deactivating effect on silver ion release even if no core–shell distribution, but homogeneous of both elements in the nanoparticle ultrastructure is present [65]. It could also be confirmed that citrate is much more potent in deactivating silver than BSA [17]. Beside this, no influence of storing laser-generated, BSA- and citrate-stabilized nanoparticle colloids over 16 weeks could be observed in comparison to the freshly prepared colloids. The precise setting of the gold–silver ratio and the homogeneous distribution of both elements within nanoparticles by laser ablation in liquid opens new chances to control the silver ion release and the biological effect by alloying on the nanoscale.

Acknowledgments We thank the German Research Foundation (DFG) for funding the priority program 1313 as well as Jan Hegermann, Manuela Kellner, and Mark Kühnel (Institute for Functional and Applied Anatomy, Medical School Hannover) for their assistance with the TEM-imaging. We would also like to thank Dennis Buchbach for his assistance in the generation of the nanoparticle colloids.

Conflicts of interest None.

References

1. Chernousova S, Epple M (2013) Silver as antibacterial agent: ion, nanoparticle, and metal. Angew Chem Int Ed Engl 52(6):1636–1653. doi:10.1002/anie.201205923
2. Daniel MC, Astruc D (2004) Gold nanoparticles: assembly, supramolecular chemistry, quantum-size-related properties, and applications toward biology, catalysis, and nanotechnology. Chem Rev 104(1):293–346
3. Saha K, Agasti SS, Kim C, Li XN, Rotello VM (2012) Gold nanoparticles in chemical and biological sensing. Chem Rev 112(5): 2739–2779
4. Chen X, Schluesener HJ (2008) Nanosilver: a nanoproduct in medical application. Toxicol Lett 176(1):1–12
5. Kim JS, Kuk E, Yu KN, Kim JH, Park SJ, Lee HJ, Kim SH, Park YK, Park YH, Hwang CY, Kim YK, Lee YS, Jeong DH, Cho MH (2007) Antimicrobial effects of silver nanoparticles. Nanomedicine 3(1):95–101
6. Feng QL, Wu J, Chen GQ, Cui FZ, Kim TN, Kim JO (2000) A mechanistic study of the antibacterial effect of silver ions on *Escherichia coli* and *Staphylococcus aureus*. J Biomed Mater Res 52(4):662–668
7. Morones JR, Elechiguerra JL, Camacho A, Holt K, Kouri JB, Ramirez JT, Yacaman MJ (2005) The bactericidal effect of silver

nanoparticles. Nanotechnology 16(10):2346–2353. doi:10.1088/0957-4484/16/10/059
8. Lu Y, Spyra P, Mei Y, Ballauff M, Pich A (2007) Composite hydrogels: robust carriers for catalytic nanoparticles. Macromol Chem Physic 208(3):254–261
9. Thomas V, Yallapu MM, Sreedhar B, Bajpai SK (2007) A versatile strategy to fabricate hydrogel–silver nanocomposites and investigation of their antimicrobial activity. J Colloid Interface Sci 315(1): 389–395. doi:10.1016/j.jcis.2007.06.068
10. Ghosh S, Kaushik R, Nagalakshmi K, Hoti SL, Menezes GA, Harish BN, Vasan HN (2010) Antimicrobial activity of highly stable silver nanoparticles embedded in agar-agar matrix as a thin film. Carbohydr Res 345(15):2220–2227. doi:10.1016/j.carres.2010.08.001
11. Grade S, Eberhard J, Wagener P, Winkel A, Sajti CS, Barcikowski S, Stiesch M (2012) Therapeutic window of ligand-free silver nanoparticles in agar-embedded and colloidal state: in vitro bactericidal effects and cytotoxicity. Adv Eng Mater 14(5):231. doi:10.1002/adem.201180016
12. Martinez-Gutierrez F, Olive PL, Banuelos A, Orrantia E, Nino N, Sanchez EM, Ruiz F, Bach H, Av-Gay Y (2010) Synthesis, characterization, and evaluation of antimicrobial and cytotoxic effect of silver and titanium nanoparticles. Nanomedicine 6(5):681–688. doi:10.1016/j.nano.2010.02.001
13. Asharani PV, Hande MP, Valiyaveettil S (2009) Anti-proliferative activity of silver nanoparticles. BMC Cell Biol 10:65. doi:10.1186/1471-2121-10-65
14. Braydich-Stolle L, Hussain S, Schlager JJ, Hofmann MC (2005) In vitro cytotoxicity of nanoparticles in mammalian germline stem cells. Toxicol Sci 88(2):412–419
15. Hussain SM, Hess KL, Gearhart JM, Geiss KT, Schlager JJ (2005) In vitro toxicity of nanoparticles in BRL 3A rat liver cells. Toxicol in Vitro 19(7):975–983. doi:10.1016/j.tiv.2005.06.034
16. Johnston HJ, Hutchison G, Christensen FM, Peters S, Hankin S, Stone V (2010) A review of the in vivo and in vitro toxicity of silver and gold particulates: particle attributes and biological mechanisms responsible for the observed toxicity. Crit Rev Toxicol 40(4):328–346. doi:10.3109/10408440903453074
17. Grade S, Eberhard J, Neumeister A, Wagener P, Winkel A, Stiesch M, Barcikowski S (2012) Serum albumin reduces the antibacterial and cytotoxic effects of hydrogel-embedded colloidal silver nanoparticles. Rsc Adv 2(18):7190–7196
18. Rath D, Barcikowski S, de Graaf S, Garrels W, Grossfeld R, Klein S, Knabe W, Knorr C, Kues W, Meyer H, Michl J, Moench-Tegeder G, Rehbock C, Taylor U, Washausen S (2013) Sex selection of sperm in farm animals: status report and developmental prospects. Reproduction 145(1):R15–R30. doi:10.1530/REP-12-0151
19. Taylor U, Barchanski A, Garrels W, Klein S, Kues W, Barcikowski S, Rath D (2012) Toxicity of gold nanoparticles on somatic and reproductive cells. Adv Exp Med Biol 733:125–133. doi:10.1007/978-94-007-2555-3_12
20. Brewer SH, Glomm WR, Johnson MC, Knag MK, Franzen S (2005) Probing BSA binding to citrate-coated gold nanoparticles and surfaces. Langmuir 21(20):9303–9307. doi:10.1021/la050588t
21. Wangoo N, Suri CR, Shekhawat G (2008) Interaction of gold nanoparticles with protein: a spectroscopic study to monitor protein conformational changes. Appl Phys Lett 92 (13): 133104
22. Rehbock C, Merk V, Gamrad L, Streubel R, Barcikowski S (2013) Size control of laser-fabricated surfactant-free gold nanoparticles with highly diluted electrolytes and their subsequent bioconjugation. Phys Chem Chem Phys 15(9):3057–3067
23. Cedervall T, Lynch I, Lindman S, Berggard T, Thulin E, Nilsson H, Dawson KA, Linse S (2007) Understanding the nanoparticle-protein corona using methods to quantify exchange rates and affinities of proteins for nanoparticles. Proc Natl Acad Sci U S A 104(7):2050–2055
24. Walczyk D, Bombelli FB, Monopoli MP, Lynch I, Dawson KA (2010) What the cell "sees" in bionanoscience. J Am Chem Soc 132(16):5761–5768
25. Liu JH, Wang AQ, Chi YS, Lin HP, Mou CY (2005) Synergistic effect in an Au–Ag alloy nanocatalyst: CO oxidation. J Phys Chem B 109(1):40–43
26. Zeng HB, Du XW, Singh SC, Kulinich SA, Yang SK, He JP, Cai WP (2012) Nanomaterials via laser ablation/irradiation in liquid: a review. Adv Funct Mater 22(7):1333–1353
27. Amendola V, Meneghetti M (2013) What controls the composition and the structure of nanomaterials generated by laser ablation in liquid solution? Phys Chem Chem Phys 15(9):3027–3046
28. Petersen S, Barcikowski S (2009) Conjugation efficiency of laser-based bioconjugation of gold nanoparticles with nucleic acids. J Phys Chem C 113:19830–19835
29. Barchanski A, Hashimoto N, Petersen S, Sajti CL, Barcikowski S (2012) Impact of spacer and strand length on oligonucleotide conjugation to the surface of ligand-free laser-generated gold nanoparticles. Bioconjug Chem 23(5):908–915
30. Wagener P, Schwenke A, Barcikowski S (2012) How citrate ligands affect nanoparticle adsorption to microparticle supports. Langmuir 28(14):6132–6140
31. Lopez-Sanchez JA, Dimitratos N, Hammond C, Brett GL, Kesavan L, White S, Miedziak P, Tiruvalam R, Jenkins RL, Carley AF, Knight D, Kiely CJ, Hutchings GJ (2011) Facile removal of stabilizer-ligands from supported gold nanoparticles. Nat Chem 3(7):551–556
32. Jakobi J, Menendez-Manjon A, Chakravadhanula VS, Kienle L, Wagener P, Barcikowski S (2011) Stoichiometry of alloy nanoparticles from laser ablation of PtIr in acetone and their electrophoretic deposition on PtIr electrodes. Nanotechnology 22(14):145601. doi:10.1088/0957-4484/22/14/145601
33. Jakobi J, Petersen S, Menendez-Manjon A, Wagener P, Barcikowski S (2010) Magnetic alloy nanoparticles from laser ablation in cyclopentanone and their embedding into a photoresist. Langmuir 26(10):6892–6897
34. Zhang JM, Oko DN, Garbarino S, Imbeault R, Chaker M, Tavares AC, Guay D, Ma DL (2012) Preparation of PtAu alloy colloids by laser ablation in solution and their characterization. J Phys Chem C 116(24):13413–13420
35. Lee I, Han SW, Kim K (2001) Production of Au–Ag alloy nanoparticles by laser ablation of bulk alloys. Chem Commun (Camb) 18: 1782–1783
36. Menendez-Manjon A, Schwenke A, Steinke T, Meyer M, Giese U, Wagener P, Barcikowski S (2013) Ligand-free gold–silver nanoparticle alloy polymer composites generated by picosecond laser ablation in liquid monomer. Appl Phys a-Mater 110(2):343–350
37. Alissawi N, Zaporojtchenko V, Strunskus T, Kocabas I, Chakravadhanula VSK, Kienle L, Garbe-Schonberg D, Faupel F (2013) Effect of gold alloying on stability of silver nanoparticles and control of silver ion release from vapor-deposited Ag-Au/polytetrafluoroethylene nanocomposites. Gold Bull 46(1):3–11
38. Hahn A, Fuhlrott J, Loos A, Barcikowski S (2012) Cytotoxicity and ion release of alloy nanoparticles. J Nanopart Res 14 (1)
39. Menendez-Manjon A, Jakobi J, Schwabe K, Krauss J, Barcikowski S (2009) Mobility of nanoparticles generated by femtosecond laser ablation in liquids and its application to surface patterning. J Laser Micro / Nanoengineering 4(2):95–99
40. Nachev P, van 'T Zand DD, Coger V, Wagener P, Reimers K, Vogt PM, Barcikowski S, Pich A (2012) Synthesis of hybrid microgels by coupling of laser ablation and polymerization in aqueous medium. J Laser Appl 24 (4):042012
41. Glover RD, Miller JM, Hutchison JE (2011) Generation of metal nanoparticles from silver and copper objects: nanoparticle dynamics on surfaces and potential sources of nanoparticles in the environment. ACS Nano 5(11):8950–8957

42. Kittler S, Greulich C, Diendorf J, Köller M, Epple M (2010) Toxicity of silver nanoparticles increases during storage because of slow dissolution under release of silver ion. Chem Mater 22: 4548–4554
43. Sjogren G, Sletten G, Dahl JE (2000) Cytotoxicity of dental alloys, metals, and ceramics assessed by millipore filter, agar overlay, and MTT tests. J Prosthet Dent 84(2):229–236. doi:10.1067/mpr.2000.107227
44. Barsch N, Jakobi J, Weiler S, Barcikowski S (2009) Pure colloidal metal and ceramic nanoparticles from high-power picosecond laser ablation in water and acetone. Nanotechnology 20(44):445603
45. Petersen S, Barcikowski S (2009) In situ bioconjugation: Single-step approach to tailored nanoparticle-bioconjugates by ultrashort pulsed laser ablation. Adv Funct Mater 19:1–6
46. Garza-Ocanas L, Ferrer DA, Burt J, Diaz-Torres LA, Ramirez Cabrera M, Rodriguez VT, Lujan Rangel R, Romanovicz D, Jose-Yacaman M (2010) Biodistribution and long-term fate of silver nanoparticles functionalized with bovine serum albumin in rats. Metallomics 2(3):204–210. doi:10.1039/b916107d
47. Ravindran A, Singh A, Raichur AM, Chandrasekaran N, Mukherjee A (2010) Studies on interaction of colloidal Ag nanoparticles with bovine serum albumin (BSA). Colloids Surf B Biointerfaces 76(1):32–37. doi:10.1016/j.colsurfb.2009.10.005
48. Tsai DH, DelRio FW, Keene AM, Tyner KM, MacCuspie RI, Cho TJ, Zachariah MR, Hackley VA (2011) Adsorption and conformation of serum albumin protein on gold nanoparticles investigated using dimensional measurements and in situ spectroscopic methods. Langmuir 27(6):2464–2477
49. Besner S, Meunier M (2010) Femtosecond laser synthesis of AuAg nanoalloys: photoinduced oxidation and ions release. J Phys Chem C 114(23):10403–10409
50. Mahl D, Diendorf J, Ristig S, Greulich C, Li ZA, Farle M, Koller M, Epple M (2012) Silver, gold, and alloyed silver–gold nanoparticles: characterization and comparative cell-biologic action. J Nanopart Res 14(10):1–10
51. Boote B, Byun H, Kim J-H (2013) One-pot synthesis of various Ag–Au bimetallic nanoparticles with tunable absorption properties at room temperature. Gold Bull 46(3):185–193. doi:10.1007/s13404-013-0099-4
52. Wagener P, Ibrahimkutty S, Menzel A, Plech A, Barcikowski S (2013) Dynamics of silver nanoparticle formation and agglomeration inside the cavitation bubble after pulsed laser ablation in liquid. Phys Chem Chem Phys 15(9):3068–3074
53. Ibrahimkutty S, Wagener P, Menzel A, Plech A, Barcikowski S (2012) Nanoparticle formation in a cavitation bubble after pulsed laser ablation in liquid studied with high time resolution small angle X-ray scattering. Appl Phys Lett 101 (10):103104
54. Lewinski N, Colvin V, Drezek R (2008) Cytotoxicity of nanoparticles. Small 4(1):26–49. doi:10.1002/smll.200700595
55. Murawala P, Phadnis SM, Bhonde RR, Prasad BL (2009) In situ synthesis of water dispersible bovine serum albumin capped gold and silver nanoparticles and their cytocompatibility studies. Colloids Surf B Biointerfaces 73(2):224–228. doi:10.1016/j.colsurfb.2009.05.029
56. Xiu ZM, Zhang QB, Puppala HL, Colvin VL, Alvarez PJJ (2012) Negligible particle-specific antibacterial activity of silver nanoparticles. Nano Lett 12(8):4271–4275
57. Sotiriou GA, Pratsinis SE (2010) Antibacterial activity of nanosilver ions and particles. Environ Sci Technol 44(14):5649–5654
58. Pillai ZS, Kamat PV (2004) What factors control the size and shape of silver nanoparticles in the citrate ion reduction method? J Phys Chem B 108(3):945–951
59. Li T, Albee B, Alemayehu M, Diaz R, Ingham L, Kamal S, Rodriguez M, Bishnoi SW (2010) Comparative toxicity study of Ag, Au, and Ag–Au bimetallic nanoparticles on *Daphnia magna*. Anal Bioanal Chem 398(2):689–700. doi:10.1007/s00216-010-3915-1
60. Hahn A, Gunther S, Wagener P, Barcikowski S (2011) Electrochemistry-controlled metal ion release from silicone elastomer nanocomposites through combination of different metal nanoparticles. J Mater Chem 21(28):10287–10289
61. Alissawi N, Zaporojtchenko V, Strunskus T, Hrkac T, Kocabas I, Erkartal B, Chakravadhanula VSK, Kienle L, Grundmeier G, Garbe-Schonberg D, Faupel F (2012) Tuning of the ion release properties of silver nanoparticles buried under a hydrophobic polymer barrier. J Nanopart Res 14 (7):928
62. Carlson C, Hussain SM, Schrand AM, Braydich-Stolle LK, Hess KL, Jones RL, Schlager JJ (2008) Unique cellular interaction of silver nanoparticles: size-dependent generation of reactive oxygen species. J Phys Chem B 112(43):13608–13619. doi:10.1021/jp712087m
63. Nel AE, Madler L, Velegol D, Xia T, Hoek EM, Somasundaran P, Klaessig F, Castranova V, Thompson M (2009) Understanding biophysicochemical interactions at the nano-bio interface. Nat Mater 8(7):543–557. doi:10.1038/nmat2442
64. Berry CC, de la Fuente JM, Mullin M, Chu SW, Curtis AS (2007) Nuclear localization of HIV-1 tat functionalized gold nanoparticles. IEEE Trans Nanobioscience 6(4):262–269
65. Tiedemann D, Taylor U, Rehbock C, Jakobi J, Klein S, Kues WA, Barcikowski S, Rath D (2013) Reprotoxicity of gold, silver, and gold-silver alloy nanoparticles on mammalian gametes. Analyst. doi:10.1039/c3an01463k